11th International Symposium on Turbulence and Shear Flow Phenomena (TSFP11)
Southampton, UK, July 30 to August 2, 2019

ONE-DIMENSIONAL TURBULENCE MODELLING OF A LIFTED METHANE/AIR JET FLAME IN A VITIATED COFLOW

Tommy Starick
Chair of Numerical Fluid and Gas Dynamics
BTU Cottbus-Senftenberg
Siemens-Halske-Ring 14,
D-03046 Cottbus, Germany
Tommy.Starick@b-tu.de

Heiko Schmidt
Chair of Numerical Fluid and Gas Dynamics
BTU Cottbus-Senftenberg
Siemens-Halske-Ring 14,
D-03046 Cottbus, Germany
Heiko.Schmidt@b-tu.de

David O. Lignell
Dept. of Chemical Engineering
Brigham Young University
Provo, UT, 84602, USA
davidlignell@byu.edu

ABSTRACT

The present preliminary numerical study investigates a lifted methane/air jet flame in a vitiated coflow by means of the map-based, stochastic One-Dimensional Turbulence (ODT) model. In the considered configuration, a jet flame issues from a central nozzle into a vitiated coflow of hot combustion products from an array of lean H_2/air flames. Centreline profiles for mixture fraction, temperature and mass fraction of O_2 and OH obtained from ODT simulations with a planar and cylindrical formulation are shown and compared to measurements from Cabra *et al.* (2005). Additionally, two-dimensional renderings of the flame and scatter plots of temperature versus mixture fraction are provided and compared to the available measurement data. Although the application of ODT for reactive flows in jet configurations is not novel, the chosen lifted jet flame in a vitiated coflow represents a challenge for the model. The accurate representation of the subtle interactions of the hot coflow products with the cold unburnt jet flow are crucial for the reaction and autoignition of the jet (Cabra *et al.*, 2005). Considering the reduced order of the model and the taken assumptions, the achieved results reasonably match with the measurement data.

INTRODUCTION & ODT FORMULATION

Clear understanding of flame extinction and stabilisation has a central importance and is usually addressed by simplified jet flames. Vitiated coflow burners allow detailed insights and investigations of the underlying extinction and flame stabilisation dynamics for lifted jet flames in an environment of hot combustion products. The simple configuration of a jet flame in a coaxial flow of hot combustion products exhibits similar characteristics for chemical kinetics, heat transfer and molecular transport as recirculation burners, while avoiding their complex recirculating fluid mechanics (Cabra *et al.*, 2002).

In this work, we address the study of the dynamics of a lifted methane/air jet flame in a vitiated coflow of hot combustion products from an array of lean H_2/air flames by means of the One-Dimensional Turbulence (ODT) model. For this purpose, we use both a planar and a cylindrical temporal ODT formulation. This section describes only the cylindrical temporal formulation as in Lignell *et al.* (2018). The description of the planar formulation can be found in Lignell *et al.* (2013).

The ODT model was formulated by A. Kerstein (Kerstein, 1999). It is an efficient approach for turbulent flow simulations, resolving all time and length scales along a notional line of sight crossing the turbulent flow field. The key advantage of ODT in comparison to filtered simulation approaches such as Reynolds-Averaged Navier-Stokes (RANS) or Large Eddy Simulations (LESs) is that it incorporates molecular processes (like chemical reactions and diffusive transport) without introducing additional approximations or modelling assumptions.

The effects of 3-D turbulence are incorporated in ODT directly by modelling the characteristics of the turbulent transport on the fluid properties along the simulated 1-D domain. This is implemented by means of stochastic 1-D eddy events. An eddy event perturbs any of the property fields by the application of a triplet map. A triplet map takes a line segment $[r_0, r_0 + l]$ with a randomly sampled eddy location r_0 and size l, shrinks it to a third of its original length, and then places three copies on the original domain. The middle copy is reversed, which ensures the continuity of advected fields and leads to a steepening of local property gradients (Lignell *et al.*, 2018).

These eddy events are sampled in time as a Poisson process using a presumed Probability Density Function (PDF) for eddy locations r_0 and sizes l. On average, this process is able to replicate the statistics of turbulent flows by oversampling the number of events modelling the turbulent transport, and maintaining a target mean acceptance

probability of eddy events (McDermott, 2005; Lignell *et al.*, 2018). In order to calculate the acceptance probability of an individual eddy in a given sampling time interval Δt_{samp}, we require the eddy rate of the event candidate λ. The latter is defined on the basis of a dimensional analysis. λ is a function of r_0, l and the eddy event time scale τ, which scales with the difference between the available kinetic energy E_{kin} in the eddy range and a viscous penalty suppression E_{vp} for small eddies, following Lignell *et al.* (2018). The latter term has no significant effect on the statistical results, but affects the performance of the model. λ is given by:

$$\lambda(l, r_0, \tau) \equiv \frac{C}{l^2 \tau} \sim C\left(E_{kin} - Z E_{vp}\right) \tag{1}$$

Here, C and Z are non-dimensional ODT model parameters which are calibrated for a specific flow configuration. Large scale coherent information is absent in ODT due to its reduced dimensionality. The sampling process may occasionally accept an unphysically large eddy, which may adversely affect the turbulent transport. This is prevented by a large eddy suppression mechanism based on the elapsed simulation time. This suppresses eddies which have a characteristic τ proportionally larger than the simulation time t. That is, eddies are only implemented if

$$\tau \leq \beta t \tag{2}$$

the condition in Eq. 2 is fulfilled, where β is another ODT model parameter which must be calibrated beforehand (Lignell *et al.*, 2018). Eddies are sampled sequentially in time. When an eddy is implemented, a deterministic advancement process of diffusive-reactive transport equations for momentum and scalar components is evolved which catches up to the time of the event implementation. In an open system configuration such as the lifted jet flame studied in this work, the deterministic advancement is governed by integral conservation laws following a Lagrangian ODT formulation as in Lignell *et al.* (2018).

Next we list the integral expressions for conservation of mass, momentum, and energy, the latter being represented by the conservation of enthalpy for open systems in a low Mach number limit approximation. The mass conservation equation is given by:

$$\frac{\mathrm{d}}{\mathrm{d}t} \int \rho r \mathrm{d}r = 0 \tag{3}$$

Here, ρ is the density of the gas mixture, which is correlated with the pressure, temperature and molecular weight of the mixture given by the ideal gas law.

$$P = \rho R_u T \sum_k \frac{Y_k}{M_k} \tag{4}$$

Here, P is the thermodynamic pressure, which remains temporally and spatially homogeneous in the open jet configuration. Also, R_u is the universal gas constant, T is the temperature of the gas mixture and Y_k and M_k are the different mass fractions and molecular weights of the k species forming the gas mixture. Species conservation is given by:

$$\frac{\mathrm{d}}{\mathrm{d}t} \int \rho Y_k r \mathrm{d}r = -\int \frac{1}{r} \frac{\partial}{\partial r} \left(\rho V_k Y_k\right) r \mathrm{d}r + \int \dot{w}_k r \mathrm{d}r \tag{5}$$

In Eq. 5, V_k are the species diffusion velocities, which require some modelling approximation as in any reactive DNS. Similarly, $\dot{w}_k$ are the species reaction rates provided by a given chemical mechanism at specified thermodynamic conditions. Next, we present the conservation of momentum. For the latter we assume dominance of radial transport and we use the gradient of scalar modelled shear stresses as those responsible for the diffusion of momentum in the system (Lignell *et al.*, 2018). The momentum transport equation is then:

$$\frac{\mathrm{d}}{\mathrm{d}t} \int \rho u_i r \mathrm{d}r = \int \frac{1}{r} \frac{\partial}{\partial r} \left(r \mu \frac{\partial u_i}{\partial r}\right) r \mathrm{d}r \tag{6}$$

Here, u_i are one of the three i velocity components in the cylindrical system. μ is the dynamic viscosity of the gas mixture. Finally, we require enthalpy h conservation given by:

$$\begin{aligned} \frac{\mathrm{d}}{\mathrm{d}t} \int \rho h r \mathrm{d}r = &-\int \frac{1}{r} \frac{\partial}{\partial r} \left(\rho V_k Y_k h_k\right) r \mathrm{d}r \\ &+ \int \frac{1}{r} \frac{\partial}{\partial r} \left(r \lambda_t \frac{\partial T}{\partial r}\right) r \mathrm{d}r \end{aligned} \tag{7}$$

Here, h_k is the sensible enthalpy of each k^{th} species and λ_t is the thermal conductivity of the mixture.

The deterministic advancement of Eq. 3-7 is done by means of a Finite Volume Method (FVM) using a first order time integration. We perform an implicit time-integration of Eq. 3-7 considering the diffusive flux terms calculated at the beginning of the time step as constants in order to remediate the potentially restrictive CFL condition due to stiff chemistry given by the species chemical reaction source term. For Eq. 6-7, however, this converts the time integration into an Explicit Euler method.

The density obtained after time stepping the enthalpy and species equations (Eq. 7 and 5) is calculated by means of Eq. 4 at the new mixture composition and temperature. After the density update, mass conservation is enforced by a conservative re-meshing of the grid following the application of Eq. 3. The fluid thermophysical properties are calculated by means of the Cantera suite software at all times (see Goodwin (2002)).

CONFIGURATION

The lifted methane/air jet flame considered is sketched in Fig. 1. The jet flame issues from a central nozzle into a vitiated coflow of hot combustion products. This coflow is created by an array of lean H_2/air flames. In the following context, r stands for the radial direction and z for the streamwise direction. In the measurement of Cabra *et al.* (2005), the coflow burners were located 70 mm below the nozzle exit. The combustion of the coflow is therefore assumed to be completed at the streamwise position of the jet outlet. In Fig. 1, the lower blue line marks the initial position of the ODT line ($z/d = 0$), whereby d stands for the jet diameter. The upper blue line illustrates a position of the ODT line after some elapsed time.

For comparison purposes, the ODT simulations consider the same parameters and setup as the experimental measurements of Cabra et al. (2005). Table 1 lists the initial conditions for the jet and coflow. Here, X are the mole

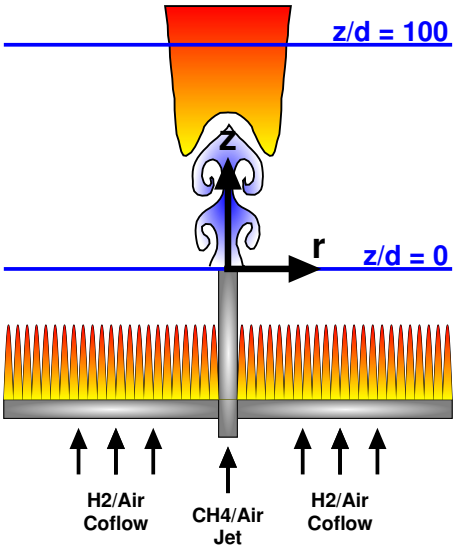

Figure 1: Schematic illustration of the lifted jet flame in a vitiated coflow

fractions of the different considered species. For the ODT simulations, the initial velocity profile of the coflow is given by a uniform distribution with a value of 5.4 m/s. The velocity profile of the jet at nozzle exit is initialised with an instantaneous velocity profile from a channel or pipe flow ODT simulation for a planar or cylindrical jet flame simulation, respectively. The ODT domain extends over a length of 100 mm with homogeneous Neumann boundary conditions at both ends. For the representation of the chemistry of the methane/air jet flame, a 19-species reduced mechanism is applied (Lu & Law, 2008).

Table 1: Initial conditions for jet and coflow used in the performed simulations.

-	Jet	Coflow
d (mm)	4.57	100
u (m/s)	100	5.4
T (K)	320	1350
X_{O_2}	0.15	0.12
X_{N_2}	0.52	0.73
X_{H_2O}	0.0029	0.15
X_{OH} (ppm)	0.0	200
X_{H_2} (ppm)	100	100
X_{CH_4}	0.33	0.0003

In this work, a comparison of preliminary ODT results from a temporal formulation with a stationary spatially developing round jet flame is intended. Since the temporal ODT formulation is solving for only one spatial direction and time, a transformation between time and their corresponding downstream position is required. Following the strategy in Echekki *et al.* (2001), the 1-D ODT line can be advected in z-direction by means of an instantaneous bulk velocity $\bar{u}$.

$$z(t) = z(t_0) + \int_{t_0}^{t} \bar{u}(t')dt' \tag{8}$$

Here, $z(t_0)$ marks the starting position. The calculation of the bulk velocity for the cylindrical ODT formulation is calculated by the sum of the free-stream (coflow) velocity u_∞ and the ratio of integrated momentum flux to integrated mass flux:

$$\bar{u}(t) = u_\infty + \left. \frac{\int_{-\infty}^{\infty} \rho (u-u_\infty)^2 r dr}{\int_{-\infty}^{\infty} \rho (u-u_\infty) r dr} \right|_t \tag{9}$$

The calculation of the bulk velocity $\bar{u}$ in the planar ODT formulation is using the same equation as in Echekki *et al.* (2001).

For all shown results, the mixture fraction definition by Bilger *et al.* (1990) is used:

$$f = \frac{2(Y_C - Y_{C,2})/M_C + (Y_H - Y_{H,2})/2M_H - (Y_O - Y_{O,2})/M_O}{2(Y_{C,1} - Y_{C,2})/M_C + (Y_{H,1} - Y_{H,2})/2M_H - (Y_{O,1} - Y_{O,2})/M_O} \tag{10}$$

Here, M denotes the elemental masses and Y the mass fractions of carbon (C), hydrogen (H), and oxygen (O). The subscripts 1 and 2 mark the jet and the coflow stream, respectively.

RESULTS

Centreline profiles provide information on the evolution of the flow and are used to validate the ODT simulation results. In Fig 2, the centreline profiles for Favre-averaged mixture fraction, temperature, mass fractions for O_2 and OH and the corresponding fluctuations for mixture fraction and temperature are shown. In all centreline plots, the red and blue curves show results from ODT simulations with a cylindrical and planar formulation, respectively. The measurement data from Cabra *et al.* (2005) is indicated by round black markers. The Favre-averaging of the ODT results is based on an ensemble of 250 realisations. For all shown results, the ODT model parameters C and Z in Eq. 1 are taken as $C = 18$ and $Z = 400$ for the cylindrical temporal ODT simulations, which are the same model parameters used in the investigations of a round jet flame with a likewise cylindrical formulation done by Lignell *et al.* (2018).

For the planar temporal ODT simulations, the model parameters are taken as $C = 5$ and $Z = 400$. A large eddy suppression is used to suppress unphysically large eddies in the beginning phase of the simulation. Here, β from Eq. 2 is taken as $\beta = 10$ for the planar and $\beta = 1.17$ for the cylindrical ODT simulations.

The initial phase in the centreline plots in Fig. 2, up to $z/d \approx 40$, is characterised by non reactive mixing between the cold jet and the hot coflow. In the initial phase, the temperature rise and oxygen consumption is low. The temperature fluctuations remain on a relatively low level and the

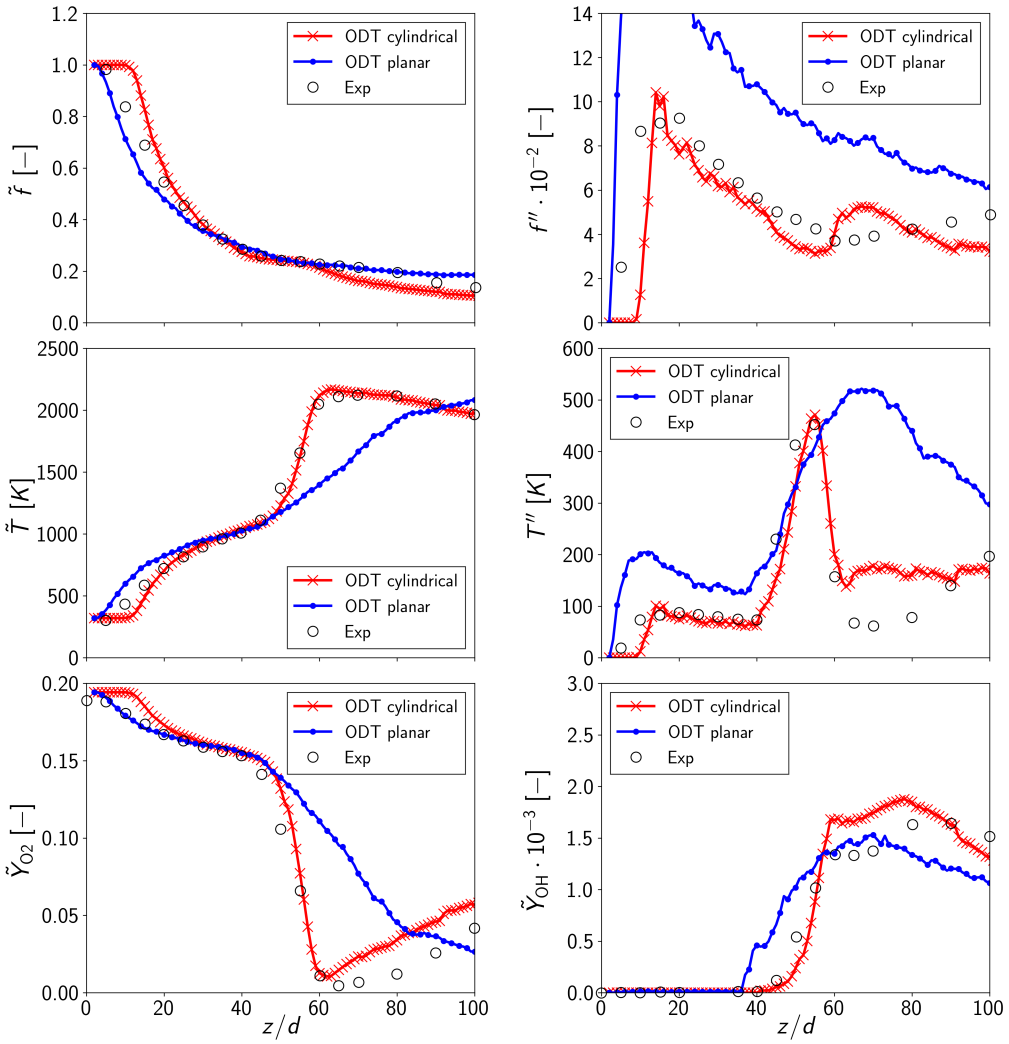

Figure 2: Comparison of centreline profiles of Favre-averaged mixture fraction ($\tilde{f}$ and fluctuations f''), temperature ($\tilde{T}$ and fluctuations T'') and species mass fractions (Favre-averaged oxygen mass fraction $\tilde{Y}_{O2}$ and Favre-averaged hydroxyl radical mass fraction $\tilde{Y}_{OH}$). Results from ODT simulations with a planar and cylindrical formulation are compared to experimental results of Cabra *et al.* (2005) (Exp).

OH mass fraction is negligible. The mixture fraction exhibits a strong decrease in the initial stage and the fluctuations reaching their maximal values. After the initial phase, a broad region of flame stabilisation follows. A strong temperature rise, rapid oxygen consumption, OH production and peak in the temperature fluctuations is typical for that region.

In the plots, the ODT results with a cylindrical formulation are in good agreement with the measurements. That includes a correct representation of the mixing in the initial phase and an accurate capture of the combustion process, which is denoted by a rapid temperature rise and oxygen mass fraction drop. ODT is also able to reproduce the trend and magnitude of the Favre fluctuations obtained in the experimental measurements. Small deviations in the Favre-averaged profiles of mixture fraction, temperature and oxygen mass fraction can be seen in the range of $z/d = 5$ to $z/d = 15$.

The planar ODT formulation reveals severe deviations to the measurement data. In the initial phase, the planar ODT formulation overpredicts the mixing and shows a higher Favre-averaged temperature and lower mixture fraction in comparison to the measurement data. The combustion process is not properly captured due to the missing temperature rise and oxygen drop. The missing temperature rise and the high level of temperature fluctuations in the region from $z/d = 50$ up to $z/d = 100$ leads to the conclusion that the planar ODT formulation predicts the point of ignition with too high fluctuations. Considering the deviations between simulation and measurements in the centreline profiles, the assumption of capturing the characteristics of a round jet flame through a planar temporal formulation is in the case considered not accurate. Therefore, the upcoming results and discussions in the rest of the paper will be done solely on the grounds of the cylindrical ODT formulation.

Fig. 3 shows scatter plots of temperature versus mixture fraction and OH mass fraction versus mixture fraction at four different axial positions. These figures are obtained by showing either the values of temperature and mixture fraction or OH mass fraction and mixture fraction obtained for each grid cell in each ensemble realisation at a given time (fixed axial position). In each plot, the dotted vertical line represents the stoichiometric mixture fraction of $f_s = 0.17$ and the dashed line non reacting conditions (pure mixing). The solid black line in the scatter plots for temperature versus mixture fraction marks equilibrium. At an

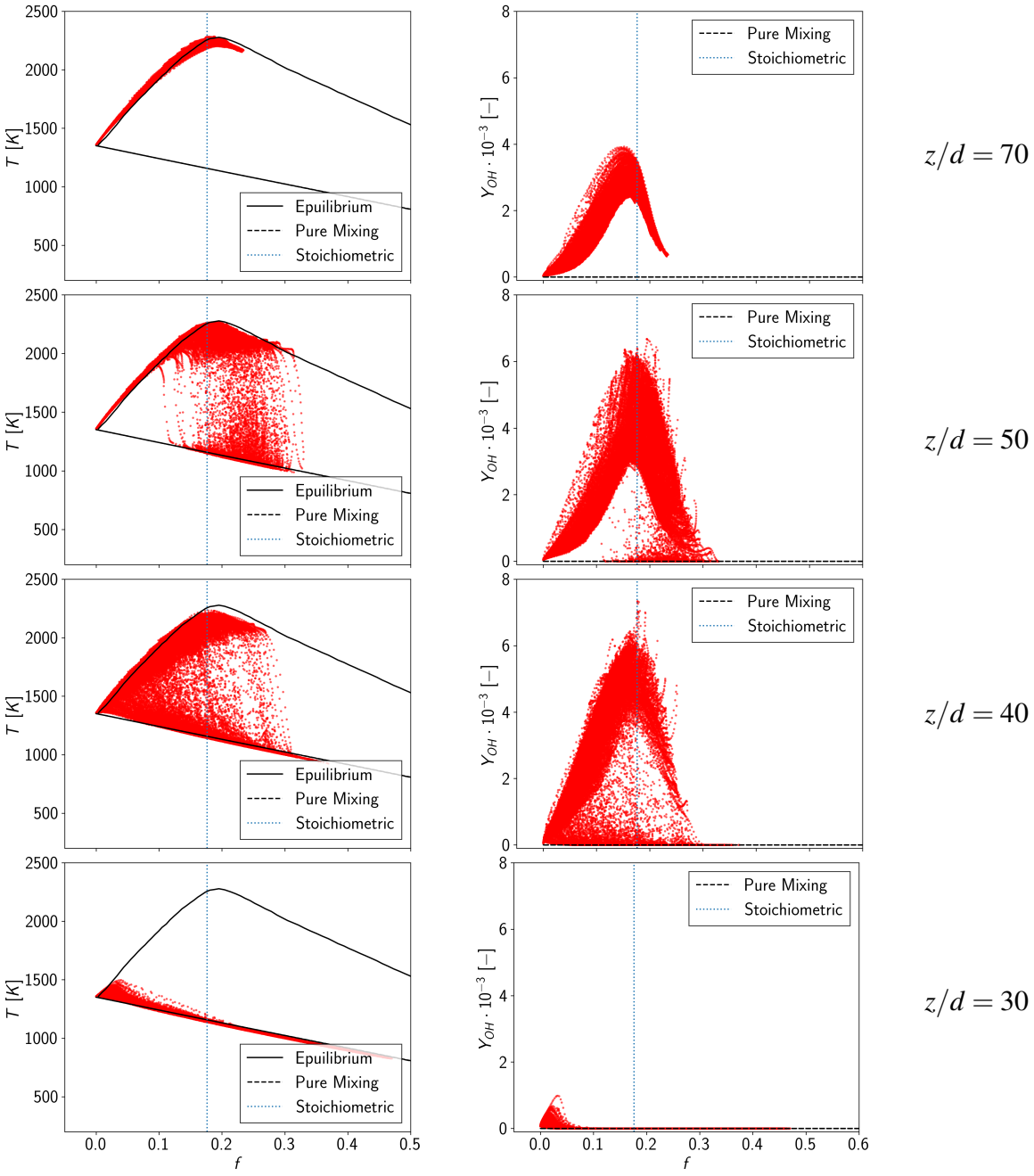

Figure 3: Scatter plots from cylindrical ODT simulations at four different axial positions. The scatter plots are showing the instantaneous distribution of temperature versus mixture fraction and OH mass fraction versus mixture fraction.

axial position of $z/d = 30$, the state is characterised by pure mixing and no reaction has started. The state of complete equilibrium is reached at an axial position of $z/d = 70$. In the scatter plots at $z/d = 40$ and $z/d = 50$, some datapoints have reached equilibrium and others are still in a condition of pure mixing without any reactions. The scatter plots are showing that ODT is able to capture the key combustion characteristics and can reproduce the scatter plots of the measurements of Cabra *et al.* (2005) (not shown here). The scattering in the ODT simulations, especially at the axial position of $z/d = 30$ and $z/d = 70$, is lower than the measurements.

Fig. 4 shows 2-D renderings of the Favre-averaged temperature, OH mass fraction and mixture fraction. Similar to the centreline profiles in Fig. 2, the initial phase is characterised by non reactive mixing. Until $z/d \approx 40$, the increase in temperature is due to the mixing with hot combustion products from the coflow. There is also no visible production of OH radicals in that specific region. The mixture fraction experiences a strong decrease due to the mixing with the coflow. After reaching $z/d = 40$, a temperature rise is seen at the interface between the coflow and jet, which is moving in the direction of the center with increasing downstream positions. The mass fraction of OH is showing a similar evolution as the temperature. High OH mass fractions occur in the region of highest temperature. The mixture fraction does not show strong changes for downstream positions $z/d > 40$.

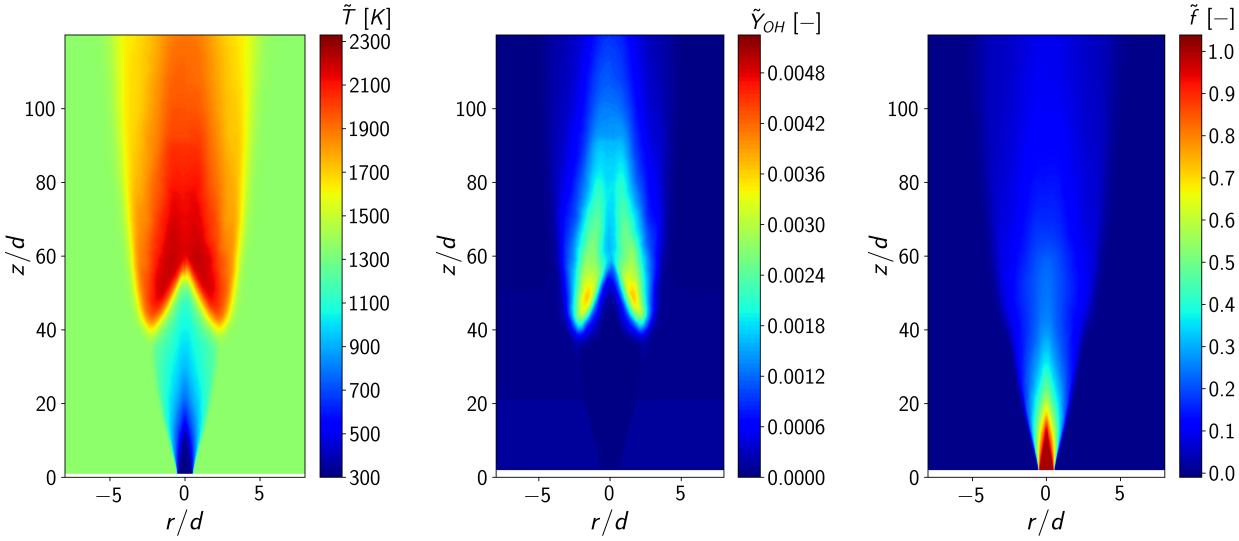

Figure 4: Two-dimensional rendering of the lifted methane/air jet flame in a vitiated coflow for the Favre-averaged temperature (left), mass fraction of OH (middle), and mixture fraction (right).

CONCLUSIONS

Preliminary ODT simulation results on a lifted methane/air jet flame in an environment of hot combustion products of a lean H_2/air flame (vitiated coflow) were presented. Two different ODT formulations were used and compared to measurement data of Cabra *et al.* (2005). The comparison of the centreline profiles from ODT simulations with a planar formulation revealed that the combustion process is not captured properly. The approximation of a round jet flame by a planar temporally evolving jet flame is therefore not correct. The comparison of the centreline profiles from ODT simulations with a cylindrical formulation with the measurement data showed a reasonable match. ODT is able to reproduce the Favre-averaged and Favre fluctuation centreline profiles. Additionally, scatter plots of temperature versus mixture fraction are presented and compared to the measurements. Here, ODT is also able to reproduce the combustion characteristics at different axial positions. The 2-D renderings of the lifted methane/air jet flame for Favre-averaged temperature, Favre-averaged OH mass fraction, and Favre-averaged mixture fraction demonstrate the capabilities of ODT in providing 2-D information from 1-D simulations. In general, the results obtained indicate that the cylindrical ODT formulation is able to capture the important combustion features of the investigated lifted jet flame in a vitiated coflow.

ACKNOWLEDGEMENTS

The authors thank Juan A. Medina M. for his contributions to the manuscript and valuable discussions. We also thank for funding by the Federal Ministry of Education and Research (BMBF) and German Academic Exchange Service (DAAD).

REFERENCES

Bilger, R.W., S.H., Stårner & R.J., Kee 1990 On Reduced Mechanisms for Methane-Air Combustion in Nonpremixed Flames. *Combustion and Flame* **80**, 135–149.

Cabra, R., Chen, J.-Y., Dibble, R. W., Karpetis, A. N. & Barlow, R. S. 2005 Lifted methane-air jet flames in a vitiated coflow. *Combustion and Flame* **143**, 491–506.

Cabra, R., Myhrvold, T., Chen, J.-Y., Dibble, R. W., Karpetis, A. N. & Barlow, R. S. 2002 Simultaneous Laser Raman-Rayleigh-LIF Measurements and Numerical Modeling Results of a Lifted Turbulent H2/N2 Jet Flame in a Vitiated Coflow. *Proc. Combust. Inst.* **29**, 1881–1888.

Echekki, T., Kerstein, A. & Dreeben, T. 2001 One-Dimensional Turbulence Simulation of Turbulent Jet Diffusion Flames: Model Formulation and Illustrative Applications. *Combustion and Flame* **125**, 1083–1105.

Goodwin, D 2002 *Cantera C++ User's Guide*. California Institute of Technology.

Kerstein, A 1999 One-dimensional turbulence: model formulation and application to homogeneous turbulence, shear flows, and buoyant stratified flows. *Journal of Fluid Mechanics* **392**, 277–334.

Lignell, D, Kerstein, A, Sun, G & Monson, E 2013 Mesh adaption for efficient multiscale implementation of One-Dimensional Turbulence. *Theoretical and Computational Fluid Dynamics* **27** (3-4), 273–295.

Lignell, D., Lansinger, V., Medina M., Juan A., Klein, M., Kerstein, A., Schmidt, H., Fistler, M. & Oevermann, M. 2018 One-dimensional turbulence modeling for cylindrical and spherical flows: model formulation and application. *Theoretical and Computational Fluid Dynamics* **32**, 495–520.

Lu, T.F. & Law, C.K. 2008 A criterion based on computational singular perturbation for the identification of quasi steady state species: A reduced mechanism for methane oxidation with NO chemistry. *Combustion and Flame* **154**, 761–774.

McDermott, R. 2005 Towards One-Dimensional Turbulence Subgrid Closure for Large-Eddy Simulation. PhD thesis, University of Utah.